Supporting Information

New ionic dinuclear Ir(III) complexes with aggregation-induced phosphorescent emission (AIPE)

Guangfu Li[a], Yong Wu[a], Guogang Shan[a], Weilong Che[a], Dongxia Zhu*[a], Baiqiao Song[a], Likai Yan*[a], Zhongmin Su[a], Martin R. Bryce*[b]

[a]*Institute of Functional Material Chemistry, Faculty of Chemistry, Northeast Normal University, Changchun 130024, People's Repubic of China; Fax: +86-0431-85684009 Tel.: +86-431-85099108, E-mail: zhudx047@nenu.edu.cn; yanlk924@nenu.edu.cn*

[b] *Department of Chemistry, Durham University, Durham, DH1 3LE, UK E-mail: m.r.bryce@durham.ac.uk*

Table of Contents

1. Experimental - general information
2. Ancillary ligands, complex **1** and complex **2** - synthesis and characterisation
3. ^{1}H NMR, ^{13}C NMR and 2D NMR spectra of complexes **1** and **2** at room temperature
4. X-ray crystallographic data
5. Electrochemical data
6. Photophysical properties
7. Quantum Chemical Calculations
8. References

1. Experimental - general information

Materials obtained from commercial suppliers were used without further purification unless otherwise stated. All glassware, syringes, magnetic stirring bars, and needles were thoroughly dried in a convection oven. Reactions were monitored using thin layer chromatography (TLC). Commercial TLC plates were used and the spots were visualised under UV light at 254 and 365 nm. ^{1}H NMR, ^{13}C NMR and 2D NMR spectra were recorded at 25ºC on a Varian 500 MHz spectrometer, ^{13}C NMR spectra were recorded at 25ºC on a Varian 125 MHz, and TMS as internal standard. The chemical shifts (δ) are given in parts per million relative to internal standard TMS (0 ppm for ^{1}H) and DMSO-d_6 (40.0 ppm for ^{13}C). The molecular weights of the complexes were obtained by using matrix-assisted laser desorption-ionization time-of-flight (MALDI-TOF) mass spectrometry. Elemental analysis was obtained using a Flash EA1112 analyser. UV-vis absorption spectra were recorded on a Shimadzu UV-3100 spectrophotometer. Photoluminescence spectra were collected on a Shimadzu RF-5301PC spectrophotometer and Maya 2000Pro optical fiber spectrophotometer. PL efficiencies were measured with an integrating sphere (C-701, Labsphere Inc.), with a 365 nm Ocean Optics LLS-LED as the excitation source, and the laser was introduced into the sphere through the optical fiber. The excited-state lifetimes were measured by exciting the samples with 355 nm light pulses with ~3 ns pulse width from a Quanty-Ray DCR-2 pulsed Nd:YAG laser. For crystal structures of complexes **1** and **2**, the data were collected on a Bruker Smart Apex II CCD diffractometer with graphite-monochromated Mo Kα radiation (λ = 0.71073 Å) at room temperature.

2. Ancillary ligands, complexes 1 and 2 - synthesis and characterization

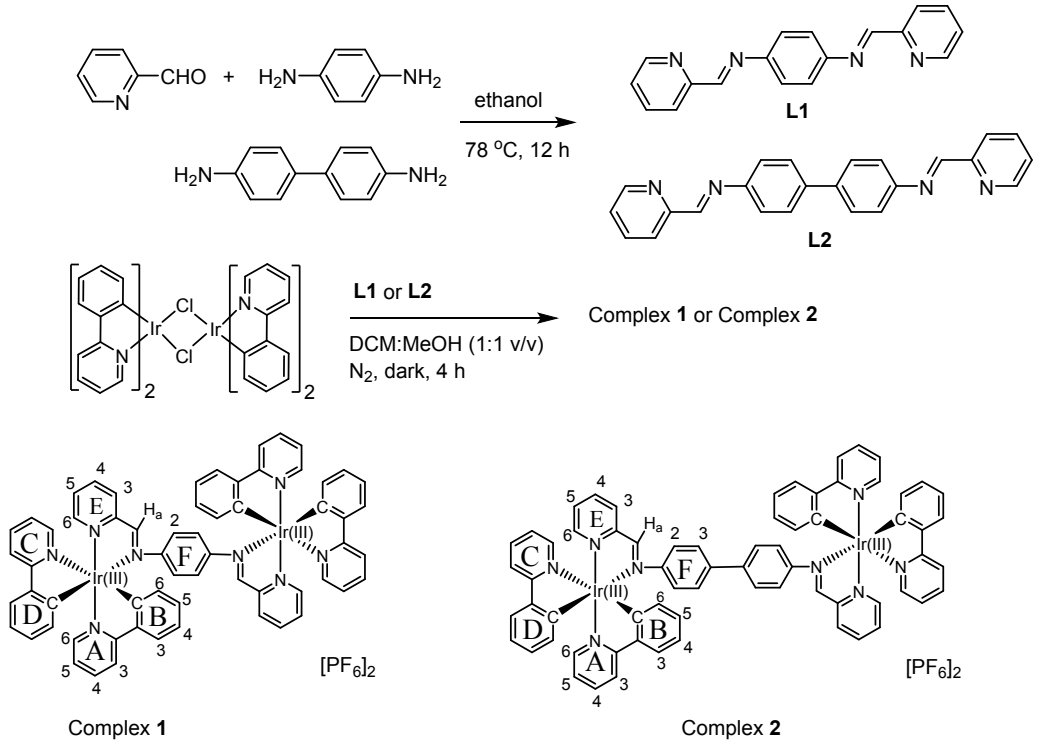

Scheme S1. The synthetic routes to the ancillary ligands **L1**, **L2**, and complexes **1** and **2**.

Synthesis of N_1,N_4-bis(pyridin-2-ylmethylene)benzene-1,4-diamine (L1)

L1 was synthesised according to the literature method.[1] 1,4-Diaminobenzene (0.108 g, 1.0 mmol) was dissolved in hot ethanol (10 ml) and 2-formylpyridine (0.214 g, 2.0 mmol) was added to the solution. Then the mixture was refluxed at 78 ^{o}C for 12 h. After cooling to room temperature a yellow precipitate quickly formed. The precipitate was then filtered and recrystallised from hot ethanol and dried in vacuo to give **L1.** Yield: 93%. ^{1}H NMR (500 MHz, CD_2Cl_2, δ [ppm]): 8.70 (d, J = 5.0 Hz, 2H), 8.66 (s, 2H), 8.20 (d, J = 8.0 Hz, 2H), 7.83 (m, 2H), 7.37 (m, 6H). MS: (MALDI-TOF) [m/z]: 286.20 (M^+) (calcd: 286.28). Anal. Calcd. for $C_{18}H_{14}N_4$: C 75.50, H 4.93, N 19.57. Found C 75.53, H 4.91, N 19.56.

Synthesis of N_4,N_4'-bis(pyridin-2-ylmethylene)-[1,1'-biphenyl]-4,4'-diamine (L2)

The synthetic procedure was the same as **L1**, except 4,4'-diaminobiphenyl was used instead of 1,4-diaminobenzene. Yield: 92%. ^{1}H NMR (500 MHz, CD_2Cl_2, δ [ppm]): 8.73 (d, J = 5.0 Hz, 2H), 8.68 (s, 2H), 8.23 (d, J = 8.0Hz, 2H), 7.83 (t, J = 8.0 Hz, 2H), 7.69 (d, J = 8.0 Hz, 4H), 7.38 (m, 6H). MS: (MALDI-TOF) [m/z]: 362.20 (M^+) (calcd: 362.23). Anal. Calcd. for $C_{24}H_{18}N_4$: C 75.54, H 5.01, N 15.45. Found C 75.57, H 5.02, N 15.41.

Synthesis of $[(ppy)_2Ir$-(L1)-$Ir(ppy)_2]$ $[PF_6]_2$ (complex 1)

A yellow suspension of the dichloro-bridged diiridium complex $[Ir(ppy)_2Cl]_2$ (0.100 g, 0.1 mmol, 1.00 eq.) and **L1** (0.029 g, 0.1 mmol, 1.00 eq.) in MeOH (15 ml) and CH_2Cl_2 (15 ml) was refluxed under an inert atmosphere of N_2 in the dark for 4 h. The red solution was then cooled to room temperature, and solid ammonium hexafluorophosphate (0.037 g, 0.2 mmol, 2.00 eq.) was added to the solution. The mixture was stirred for 45 min at room temperature and the suspension was then filtered and the precipitate was washed with petroleum ether and dried. The crude product was recrystallised from petroleum ether to yield complex **1** as a red solid (0.117 g, 86% yield). Complex **1** exists in solution as a pair of diastereoisomers. There is a slight excess of one isomer over the other (ca. 1.3:1). The major isomer is arbitrarily designated as α; the minor as β. Where separate signals are visible for the two isomers, they are reported separately, but in each case integrals are quoted relative to the molecular formula for that isomer (i.e. 1H represents one hydrogen for that isomer). ^{1}H NMR (500 MHz, DMSO-d_6, δ [ppm]): 9.42 (s, 1H, $H^{a\beta}$), 9.38 (s, 1H, $H^{a\alpha}$), 8.48-8.42 (m, 2H, $H^{E3\alpha+\beta}$), 8.34 (d, J = 6.0 Hz, 1H $H^{C6\beta}$), 8.30-8.26 (m, 4H, $H^{C3\alpha+\beta}$ and $H^{E4\alpha+\beta}$), 8.22 (d, J = 6.0 Hz, 1H, $H^{A3\beta}$), 8.18 (d, J = 6.0 Hz, 1H $H^{C6\alpha}$), 8.12 (d, J = 6.0 Hz, 1H, $H^{A3\alpha}$), 8.08 (t, J = 9.0 Hz, 1H, $H^{A4\beta}$), 8.03-7.98 (m, 3H, $H^{A4\alpha}$ and $H^{C4\alpha+\beta}$), 7.91-7.89 (d, J = 7.0 Hz, 2H, $H^{D3\alpha+\beta}$), 7.80-7.78 (m, 2H, $H^{E6\alpha+\beta}$), 7.77-7.72 (m 2H, $H^{E5\alpha+\beta}$), 7.65-7.59 (m, 2H, $H^{B3\alpha+\beta}$), 7.50 (t, J = 5.0 Hz, 2H, $H^{A6\alpha+\beta}$), 7.32-7.26 (m, 2H, $H^{C5\alpha+\beta}$), 7.23, (t, J = 7.5 Hz, 2H, $H^{A5\alpha+\beta}$), 7.01 (t, J = 7.5 Hz, 2H, $H^{D4\alpha+\beta}$), 6.89 (t, J = 7.5 Hz, 2H, $H^{D5\alpha+\beta}$), 6.85-6.79 (m, 2H, $H^{B5\alpha+\beta}$) 6.75 (t, J = 6.5 Hz, 1H, $H^{B4\beta}$), 6.70-6.65 (m, 5H, $H^{F2\alpha+\beta}$ and $H^{B4\alpha}$), 6.07 (d, J = 7.5 Hz, 2H, $H^{D6\alpha+\beta}$), 5.97 (d, J = 6.0 Hz, 2H, $H^{B6\alpha+\beta}$). ^{13}C NMR (DMSO-d_6, 125 MHz, δ[ppm]): 120.2($C^{A3\alpha+\beta}$), 120.4($C^{C3\alpha+\beta}$), 122.3($C^{B4\alpha+\beta}$), 122.4 ($C^{B5\alpha+\beta}$), 123.0($C^{D4\beta}$), 123.1($C^{D4\alpha}$), 123.2($C^{F2\beta}$), 123.3($C^{F2\alpha}$), 124.2($C^{A5\beta}$), 124.3($C^{A5\alpha}$), 124.4($C^{C5\alpha+\beta}$),

125.0($C^{B3\alpha}$), 125.1($C^{B3\beta}$), 125.5($C^{D3\alpha}$), 125.6($C^{D3\beta}$), 130.0($C^{B5\beta}$), 130.7($C^{D5\alpha+\beta}$), 130.8($C^{E5\alpha+\beta}$), 130.9($C^{D6\alpha+\beta}$), 131.2($C^{B6\alpha+\beta}$), 131.9($C^{E3\alpha+\beta}$), 139.2($C^{C4\alpha+\beta}$), 139.3($C^{A4\alpha}$), 139.4($C^{A4\beta}$), 140.2($C^{E4\alpha+\beta}$), 143.8($C^{B1\alpha}$), 143.9($C^{B1\beta}$), 144.1($C^{D1\alpha+\beta}$), 147.5($C^{F1\beta}$), 147.6($C^{F1\alpha}$), 148.6($C^{D2\alpha}$), 148.7($C^{D2\beta}$), 149.5($C^{A6\alpha+\beta}$), 149.7($C^{B2\alpha+\beta}$), 150.3($C^{E6\alpha+\beta}$), 150.9($C^{C6\alpha+\beta}$), 155.8($C^{E2\alpha+\beta}$), 166.8($C^{C2\alpha+\beta}$), 167.2($C^{A2\alpha+\beta}$), 170.6($C^{a\beta}$), 170.8($C^{a\alpha}$). MS: (MALDI-TOF) [m/z]: 1578.30 (M-PF_6) (calcd: 1578.24). Anal. Calcd. for $C_{62}H_{46}F_{12}Ir_2N_8P_2$: C 47.21, H 2.94, N 7.10. Found C 47.24, H 2.90, N 7.11. Crystals for X-ray analysis were obtained by slow evaporation of a dichloromethane-methanol solution of the complex.

Synthesis of [$(ppy)_2$Ir-(L2)-Ir$(ppy)_2$] [PF_6]$_2$ (complex 2)

The synthesis of complex **2** was similar to that of complex **1** except that the ancillary ligand **L1** was replaced by **L2**. Complex **2** was obtained as a red solid (0.130 g, 88% yield). Only one diastereoisomer is observed in solution. ^{1}H NMR (500 MHz, DMSO-d_6, δ [ppm]): 9.68 (s, 1H, H^a), 8.56 (d, J = 7.5 Hz, 1H, H^{E3}), 8.44 (d, J = 5.0 Hz, 1H, H^{C6}), 8.29 (m, 2H, H^{C3+E4}), 8.11 (d, J = 8.0 Hz, 1H, H^{A3}), 7.97 (m, 2H, H^{A4+C4}), 7.90 (d, J = 8.0 Hz, 1H, H^{D3}), 7.82 (d, J = 5.0 Hz, 1H, H^{E6}), 7.73 (t, J = 7.0 Hz, 1H, H^{E5}), 7.61 (m, 2H, H^{A6+B3}), 7.33 (m, 3H, H^{C5+F3}), 7.26 (t, J = 6.5 Hz, 1H, H^{A5}), 7.01 (m, 2H, H^{D4+F2}), 6.86 (t, J = 7.0 Hz, 1H, H^{D5}), 6.78 (t, J = 7.5 Hz, 1H, H^{B4}), 6.73 (t, J = 7.5 Hz, 1H, H^{B5}), 6.09 (d, J = 7.0 Hz, 1H, H^{D6}), 6.04 (d, J = 7.5 Hz, 1H, H^{B6}). ^{13}C NMR (DMSO-d_6, 125 MHz, δ[ppm]): 120.2(C^{A3}), 120.7(C^{C3}), 122.2(C^{B4}), 123.0($C^{D4\text{ or }F2}$), 123.7($C^{D4\text{ or }F2}$), 124.3(C^{A5}), 124.6($C^{C5\text{ or }F3}$), 125.1(C^{B3}), 125.5(C^{D3}), 127.0($C^{C5\text{ or }F3}$), 130.2(C^{B5}), 130.7(C^{D5}), 130.8(C^{E5}), 131.1(C^{D6}), 131.5(C^{B6}), 131.8(C^{E3}), 138.7(C^{F4}), 139.4(C^{C4}), 139.4(C^{A4}), 140.3(C^{E4}), 143.9(C^{B1}), 144.1(C^{D1}), 147.8(C^{F1}), 149.1(C^{D2}), 149.9(C^{A6}), 150.4(C^{E6}), 150.7(C^{B2}), 151.3(C^{C6}), 156.0(C^{E2}), 166.9(C^{C2}), 167.4(C^{A2}), 170.2(C^a). MS: (MALDI-TOF) [m/z]: 1654.30 (M-PF_6) (calcd: 1654.27). Anal. Calcd. for $C_{68}H_{50}F_{12}Ir_2N_8P_2$: C 49.39, H 3.05, N 6.78. Found C 49.41, H 3.02, N 6.79. Crystals for X-ray analysis were obtained by slow evaporation of a dichloromethane-methanol solution of the complex.

3. ^{1}H NMR and ^{13}C NMR spectra of complexes 1 and 2 at room temperature

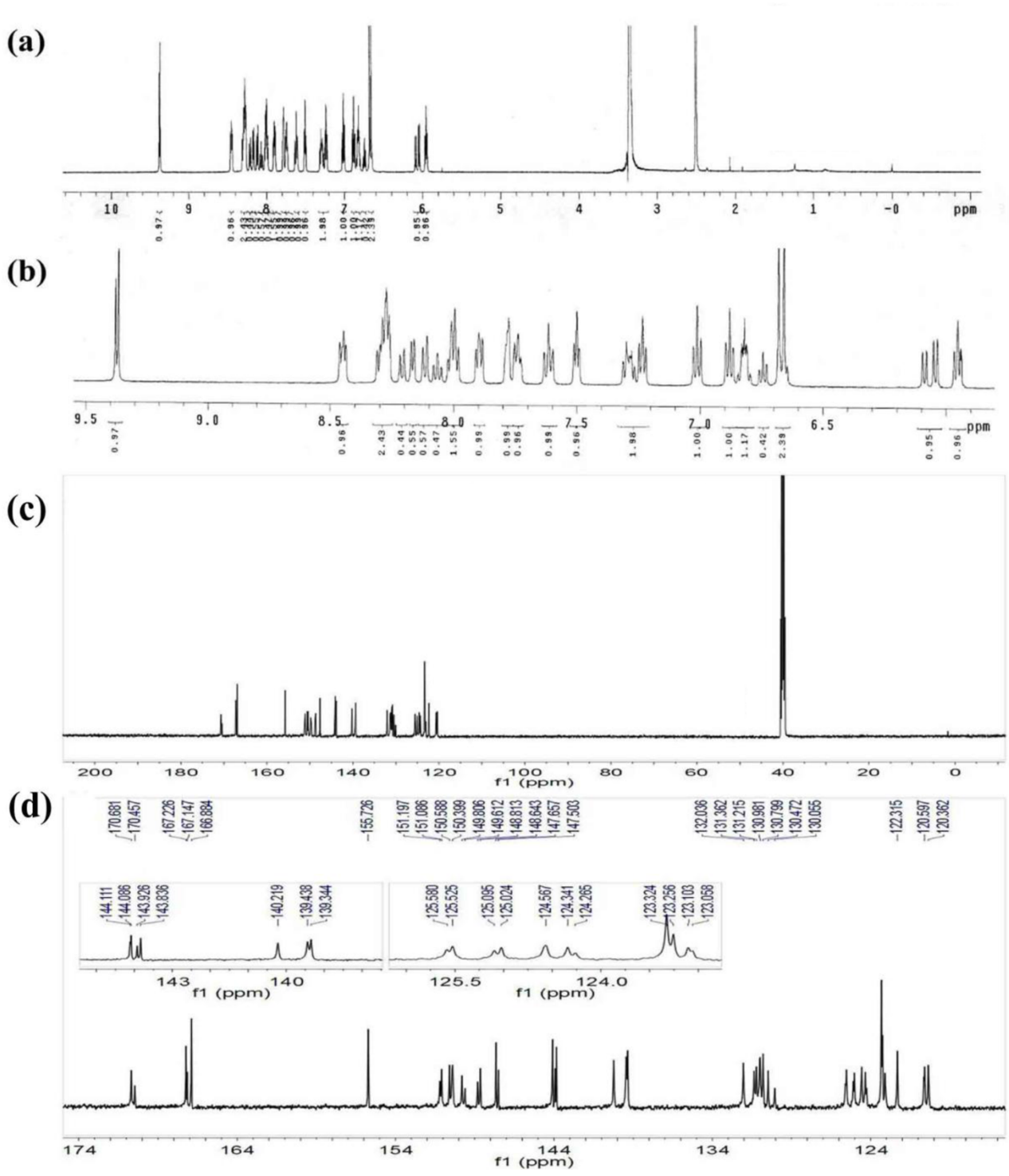

Fig. S1 (a) ^{1}H NMR spectrum of complex **1** in DMSO-d_6. (b) Expansion of the aromatic region for complex **1**. (c) ^{13}C NMR spectrum of complex **1** in DMSO-d_6. (d) Expansion of the aromatic region for complex **1**.

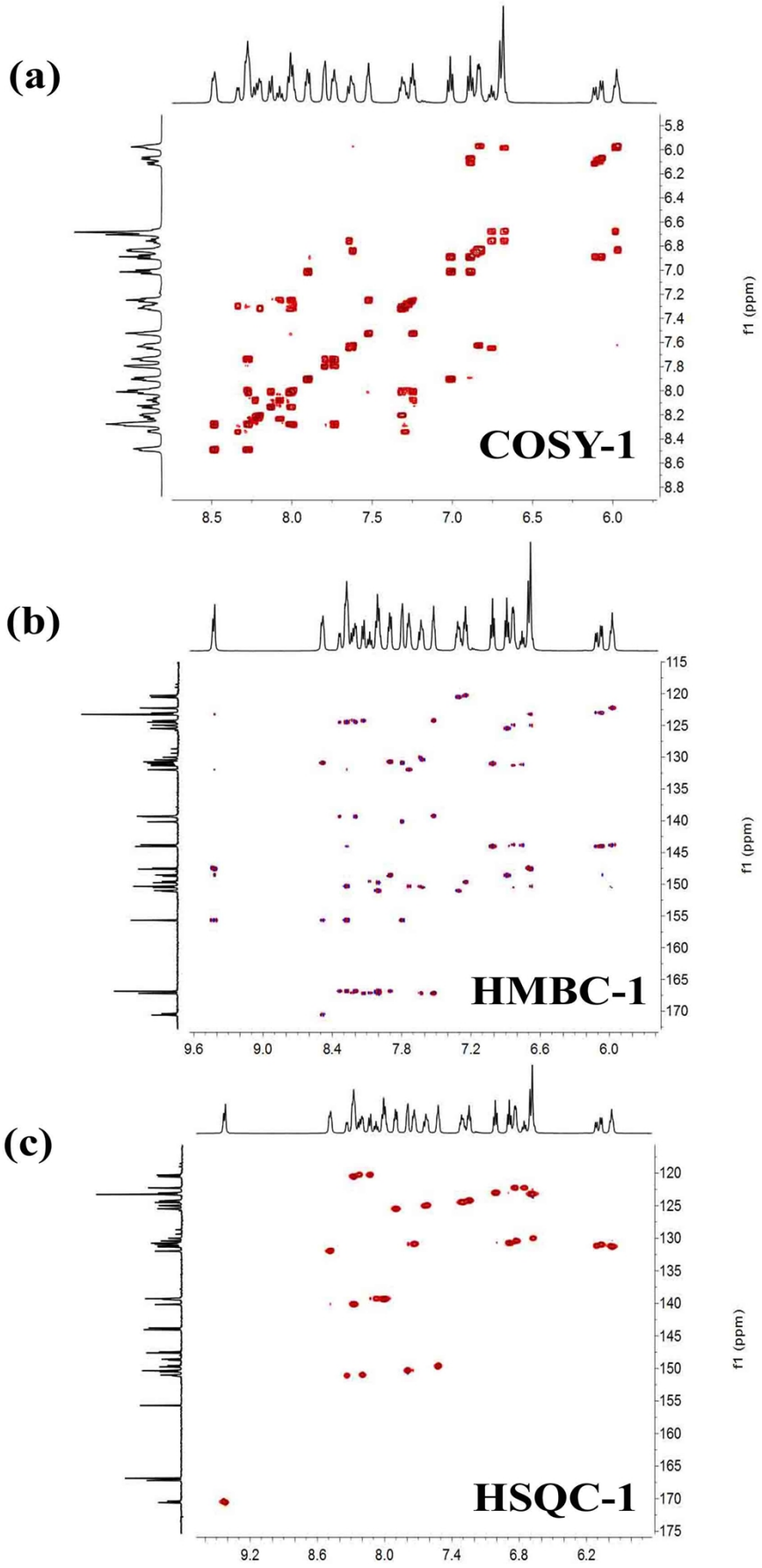

Fig. S2 (a) 2D COSY NMR spectrum of complex **1** in DMSO-d_6. (b) 2D HMBC

NMR spectrum of complex **1** in DMSO-d_6. (c) 2D HSQC NMR spectrum of complex **1** in DMS O-d_6.

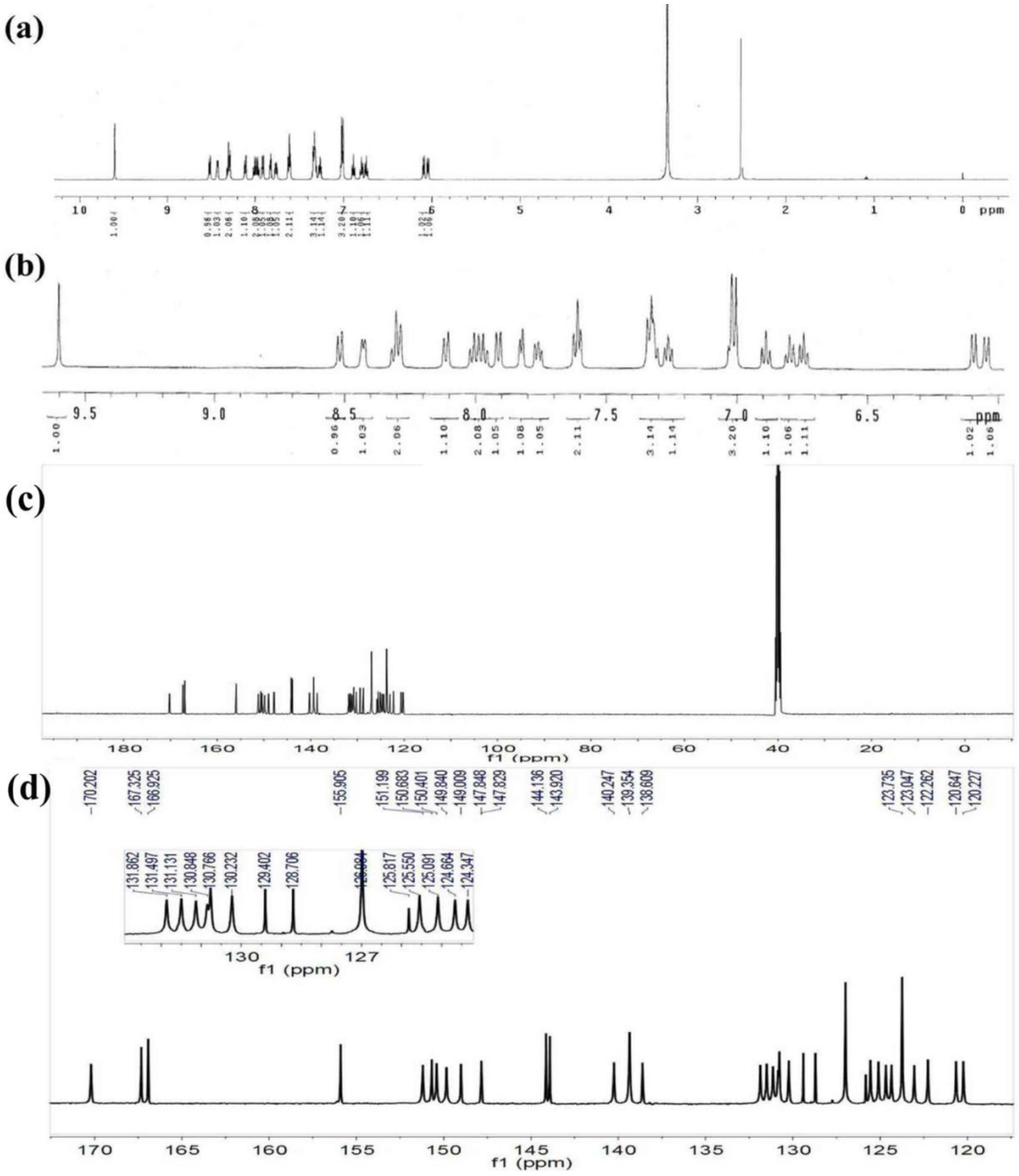

Fig. S3 (a) ^{1}H NMR spectrum of complex **2** in DMSO-d_6. (b) Expansion of the aromatic region for complex **2**. (c) ^{13}C NMR spectrum of complex **2** in DMSO-d_6. (d) Expansion of the aromati c region for complex **2**.

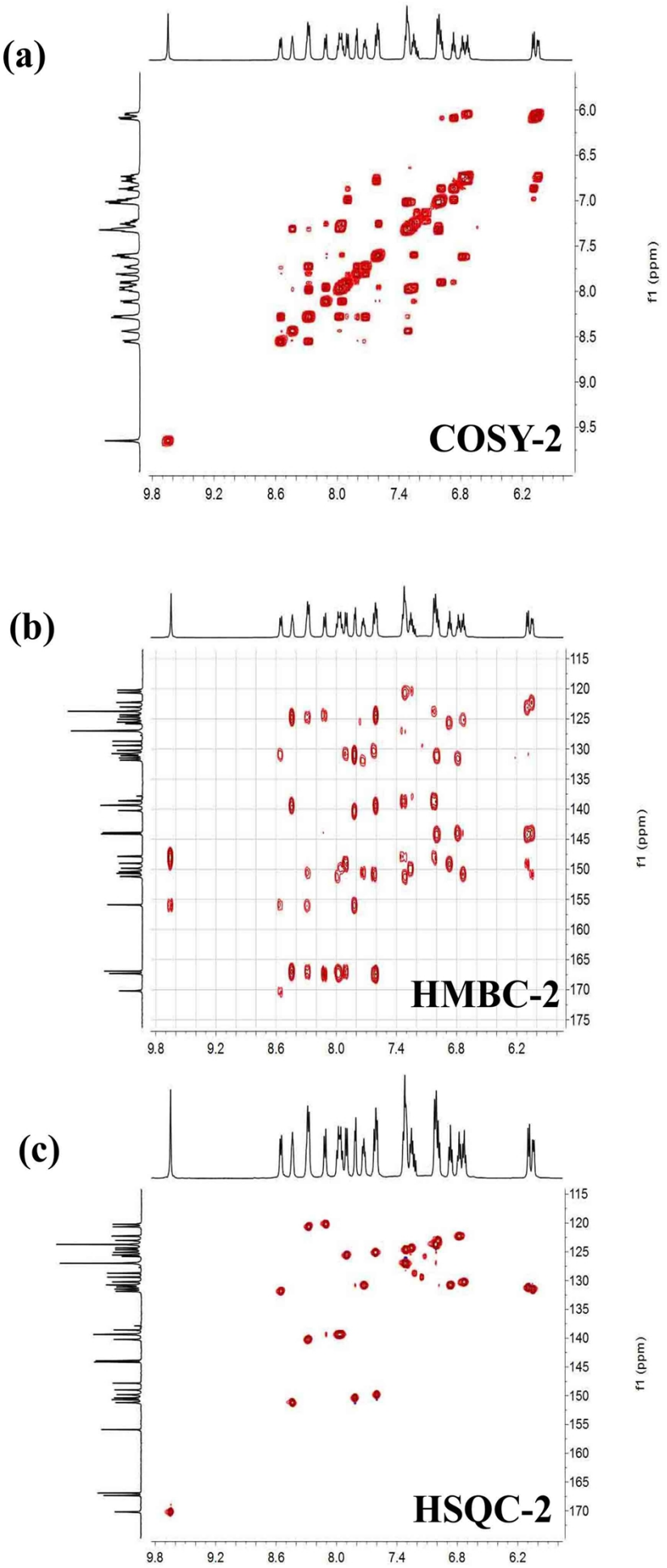

Fig. S4 (a) 2D COSY NMR spectrum of complex **2** in DMSO-d_6. (b) 2D HMBC NMR spectrum of complex **2** in DMSO-d_6. (c) 2D HSQC NMR spectrum of complex **2** in DMSO-d_6.

4. X-ray crystallography data

The molecular structures of complexes **1** and **2** were confirmed by X-ray crystallographic analysis of single crystals obtained by slow evaporation of a dichloromethane-methanol (3:1 v/v) solution of the complex **2**. Diffraction data were collected on a Bruker SMART Apex CCD diffractometer using k(Mo-K) radiation (k = 0.71073 Å). Cell refinement and data reduction were made by the SAINT program. The structure was determined using the SHELXTL/PC program. All non-hydrogen atoms were refined anisotropically, whereas hydrogen atoms were placed at the calculated positions and included in the final stage of refinements with fixed parameters. Fig. S5 shows Oak Ridge thermal ellipsoid plot (ORTEP) drawings of complexes **1** and **2**. The crystallographic data have been deposited with the Cambridge Crystallographic Data Centre with CCDC deposition numbers 976189 and 970289. These data can be obtained free of charge from The Cambridge Crystallographic Data Centre via www.ccdc.cam.ac.uk/data_request/cif.

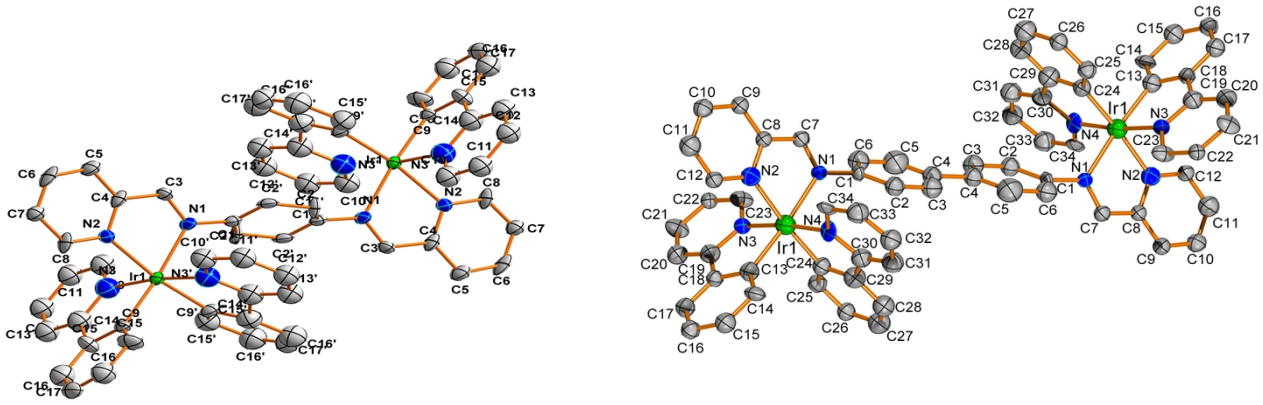

Fig. S5 The dication in the molecular structures of complexes **1** and **2** in the crystal. The H atoms, PF_6^- anions and solvent molecules are omitted for clarity.

Table S1 Crystal data and structure refinement for complex **1**.

	Complex **1**
Empirical formula	$C_{62}H_{46}F_{12}Ir_2N_8P_2$
Formula weight	1577.41
Temperature (K)	296(2)
Crystal system	Orthorhombic
space group	Cmca
a /Å	16.075(5)
b /Å	22.454(6)
c /Å	16.949(5)
α /°	90.000
β /°	90.000
γ /°	90.000
V/Å^3	6118(3)
Z	4

ρ_{calc} (g/cm^3)	1.713
μ/mm^{-1}	4.481
R_{int}	0.0656
Goodness-of-fit on F^2	1.052
R_1[a], wR_2[b] [I>2σ(I)]	0.0583, 0.1607
R_1, wR_2 (all data)	0.0832, 0.1772

[a] $R_1 = \Sigma||Fo| - |Fc||/\Sigma|Fo|$. [b] $wR_2 = \{ \Sigma[w(Fo^2 - Fc^2)^2]/ \Sigma[w(Fo^2)^2]\}^{1/2}$

Table S2 Crystal data and structure refinement for complex **2**.

	Complex **2**
Empirical formula	$C_{68}H_{50}F_{12}Ir_2N_8P_2$
Formula weight	1653.50
Temperature (K)	293(2)
Crystal system	Monoclinic
space group	p2(1)/c
a /Å	8.8497(18)
b /Å	29.644(6)
c /Å	13.885(3)
α /°	90.000
β /°	91.47(3)
γ /°	90.000
V/Å^3	3641.3(13)
Z	2
ρ_{calc} (g/cm^3)	1.508
μ/mm^{-1}	3.768
R_{int}	0.0595
Goodness-of-fit on F^2	1.013
R_1[a], wR_2[b] [I>2σ(I)]	0.0546, 0.1316
R_1,wR_2 (all data)	0.0837, 0.1403

[a] $R_1 = \Sigma||Fo| - |Fc||/\Sigma|Fo|$. [b] $wR_2 = \{ \Sigma[w(Fo^2 - Fc^2)^2]/ \Sigma[w(Fo^2)^2]\}^{1/2}$

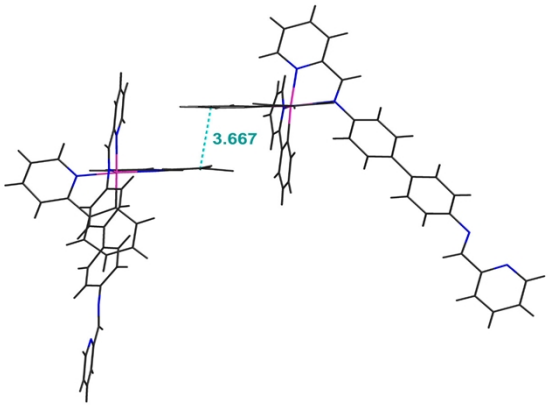

Fig. S6 Interaction between two molecules of complex **2** in the crystal.

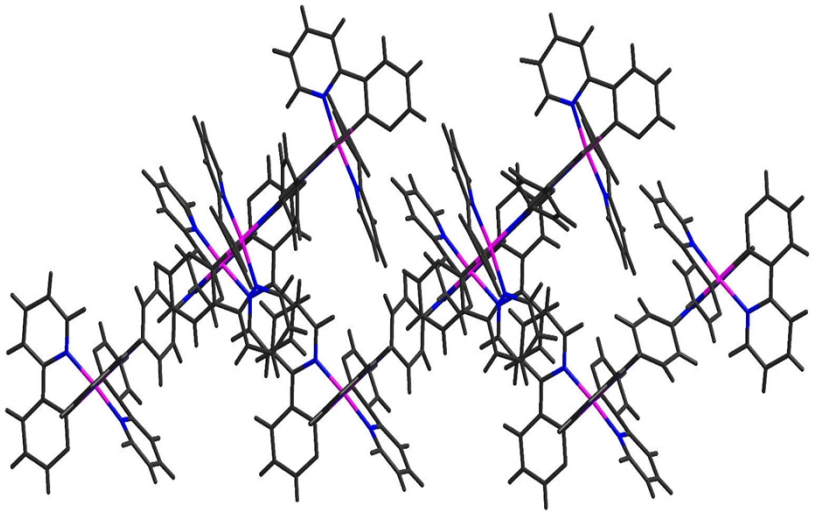

Fig. S7 Ladder-like double chain structure formed by CH··· π stacking in complex **1** in the crystal.

5. Electrochemical data

Electrochemical measurements were performed in anhydrous CH_3CN with a BAS 100 W bioanalytical electrochemical work-station, using Pt as the working electrode, platinum wire as the auxiliary electrode, and a porous glass wick (Ag/Ag^+) as the reference electrode. The data was standardised against a ferrocene/ferrocenium couple with a scan rate of 100 mV s^{-1}.

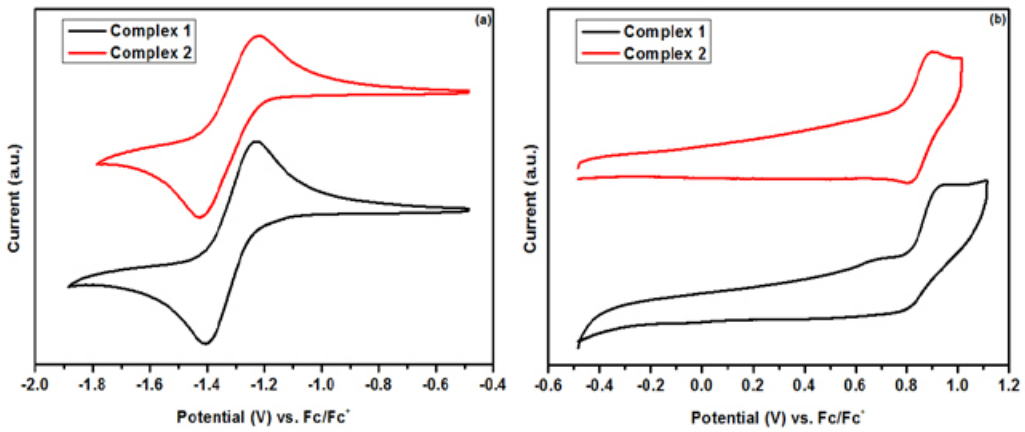

Fig. S8 Cyclic voltammograms of complexes **1** and **2** measured in acetonitrile in the presence of 0.1 M tetrabutylammonium hexafluorophosphate as supporting electrolyte with 100 mV/s scan speed. Showing (a) reduction and (b) oxidation waves.

6. Photophysical properties

Table S3 UV-Vis Absorption and Luminescence Data for **1** and **2**.

Complex	Solvent (T/K)	λ_{abs}/nm(ε/$10^{-5}M^{-1}cm^{-1}$)	λ_{em}/nm	Φ_L [a]
1	MeCN(298)	252(7835),369$_{sh}$(2310)		0.00082
	MeCN(77)		665	
	CH_2Cl_2(298)	253(8510),369$_{sh}$(2890)		
2	MeCN(298)	254(9860),376$_{sh}$(3670)		0.00071
	MeCN(77)		643,699	
	CH_2Cl_2(298)	256(9430),380$_{sh}$(3910)		

[a] Photoluminescence quantum yield(PLQY) in degassed acetonitrile solution (1×10^{-5} mol^{-1} L^{-1}), λ_{exc} = 365 nm; error for Φ_L±5% .

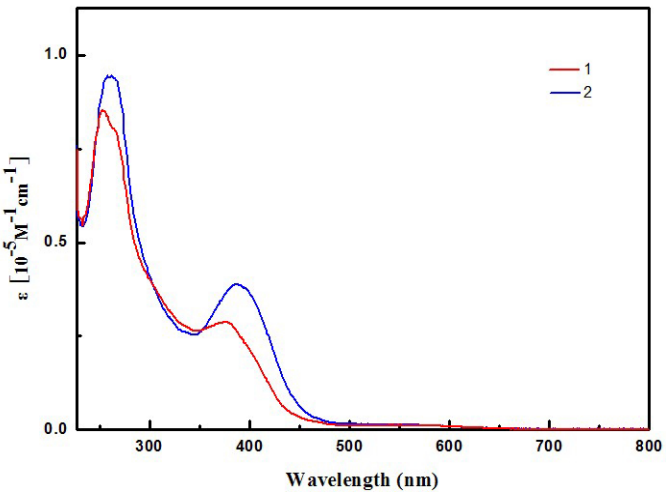

Fig. S9 UV-Vis absorption spectra of complexes **1** and **2** in CH_2Cl_2 solution (1×10^{-5} M) at room temperature.

Table S4 Emission data (λ_{max}) for complexes **1** and **2** in different states (at 298 K).

Complex	crystal	powder	film
1	694 nm	675 nm	644 nm
2	724 nm	697 nm	692 nm

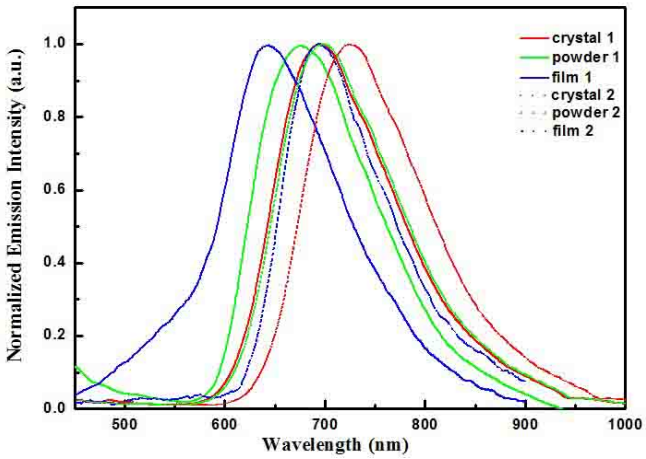

Fig. S10 Emission spectra of complexes **1** and **2** in different states at room temperature.

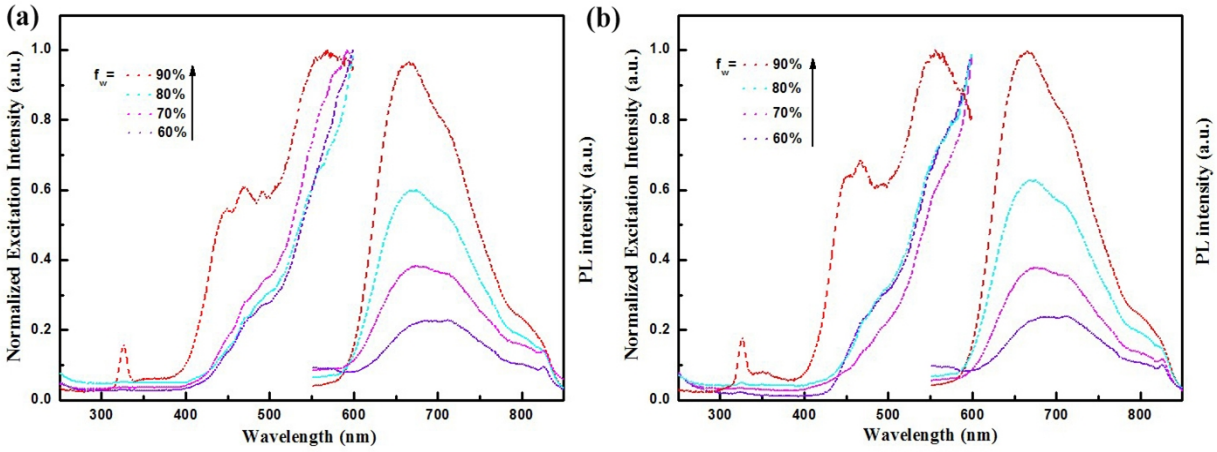

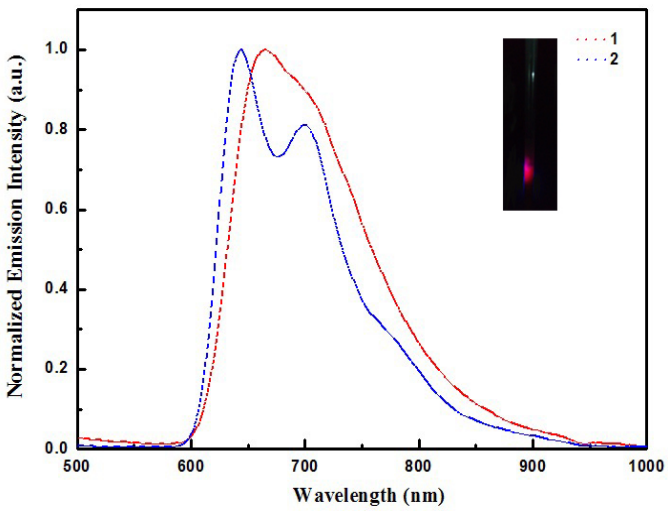

Fig. S11 Excitation and emission spectra of complexes **1 (a)** and **2 (b)** in water/CH_3CN mixtures with different water fractions (60-90% v/v) at room temperature.

Fig. S12 Emission spectra of complexes **1** and **2** in CH_3CN solution (1×10^{-5} M) at 77 K. Inset: A photograph of complex **1** emission in CH_3CN solution (1×10^{-5} M) at 77 K under UV light (365 nm) illumination.

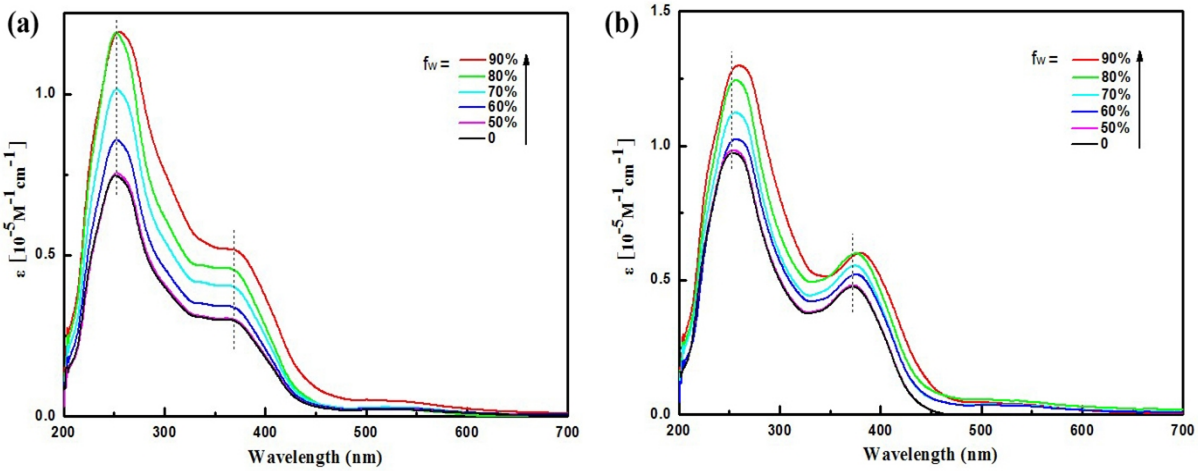

Fig. S13 (a) UV spectra of **1 (a)** and **2 (b)** in water–acetonitrile mixtures (concentration of 10 μM).

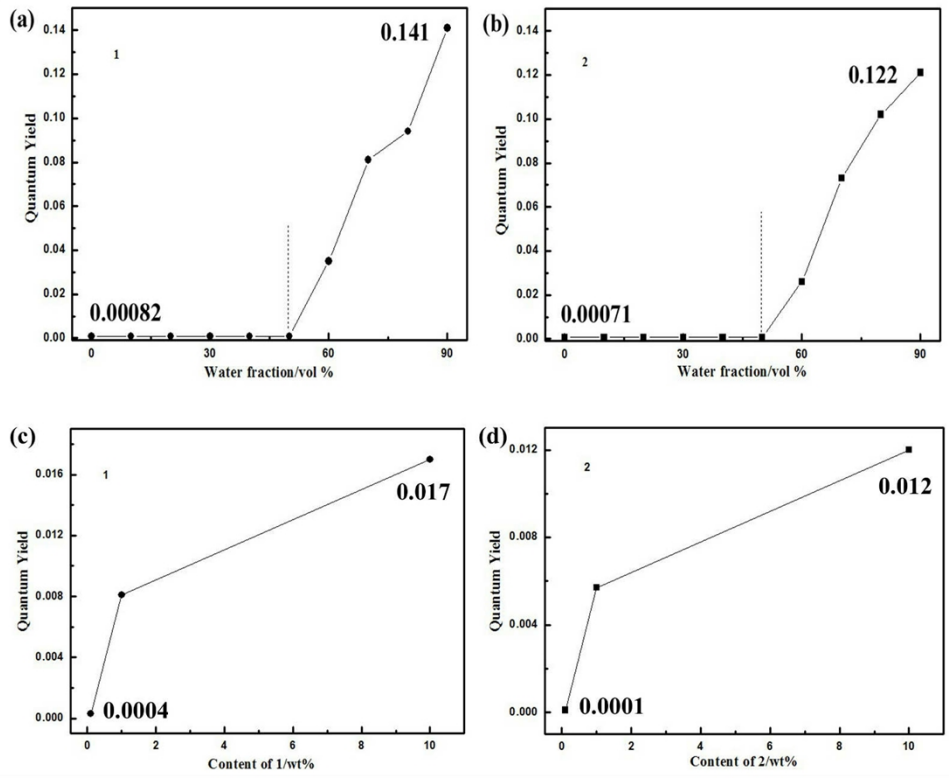

Fig. S14 (a) PL quantum yields (Φ_L) of complex **1** at 1×10^{-5} M, as a function of water fraction in a CH_3CN/water mixture (excited at 365 nm). (b) PL quantum yields (Φ_L) of complex **2** at 1×10^{-5} M, as a function of water fraction in a CH_3CN/water mixture (excited at 365 nm). (c) PL quantum yields (Φ_L) of **1**–PMMA composites (excited at 365 nm). (d) PL quantum yields (Φ_L) of **2**–PMMA composites (excited at 365 nm): error for Φ_L ±5% .

7. Quantum Chemical Calculations

All calculations were performed with Gaussian 09 program package.[2] The B3LYP functional was employed for all DFT calculations. The 6-31G* basis set was employed for H, C, N atoms, while the iridium atom was described by the Hay-Wadt effective core potential (ECP) and a double-ξ basis set LANL2DZ. Full geometry optimisation with C1 symmetry constraints was carried out in solution for the singlet ground state (S_0) of complex **2**. A solvent effect was taken into account by the polarisable continuum model (PCM) with acetonitrile as solvent. Single point calculations were performed using the crystal structure of complex **2**. TD-DFT with CAM-B3LYP was adopted to investigate the emission properties at the optimised T_1 geometry. From the electron density difference map, the T_1 states of the complexes involve transitions with the mixture of MLCT, LLCT and LC characters.

Table S5 Selected calculated bond lengths (Å), bond angles (°) and dihedral angles (°) at both optimized S_0 and T_1 geometries for complexes **1** and **2**.

	1		**2**	
	S_0	T_1	S_0	T_1
Ir1-C1	2.019	2.009	2.018	2.012
Ir1-C2	2.025	2.007	2.024	1.997
Ir1-N1	2.085	2.084	2.084	2.086
Ir1-N2	2.087	2.085	2.086	2.087
Ir1-N3	2.306	2.300	2.230	2.230
Ir1-N4	2.225	2.231	2.227	2.245
Ir2-C3	2.020	2.009	2.020	2.019
Ir2-C4	2.024	2.007	2.023	2.023
Ir2-N5	2.087	2.084	2.086	2.086
Ir2-N6	2.087	2.085	2.085	2.085
Ir2-N7	2.289	2.296	2.288	2.295
Ir2-N8	2.228	2.231	2.228	2.226
C1-Ir1-C2	87.88	89.93	88.18	91.89
C1-Ir1-N2	94.08	95.41	94.21	96.57
C2-Ir1-N3	102.75	103.20	102.58	104.58

N3-Ir1-N2	90.91	90.95	90.95	89.80
C1-Ir1-N4	95.38	92.19	95.11	88.62
N3-Ir1-N4	74.19	75.02	74.34	75.32
C1-Ir1-N3	168.91	166.22	168.75	163.12
N4-Ir1-C2	175.38	175.41	175.40	174.77
N1-Ir1-N2	172.33	174.35	172.50	175.56
C3-Ir2-C4	88.45	89.93	88.53	88.27
C3-Ir2-N6	93.93	95.41	94.09	94.30
C4-Ir2-N7	102.11	103.20	102.03	102.41
N7-Ir2-N6	91.38	90.95	91.19	91.02
C3-Ir2-N8	95.41	92.19	95.28	95.08
N7-Ir2-N8	74.27	75.02	74.37	74.47
C3-Ir2-N7	168.88	166.22	168.88	168.76
N8-Ir2-C4	174.94	175.41	175.17	175.34
N5-Ir2-N6	172.20	174.34	172.37	172.55
C5-N3-C6-C7	37.37	25.58	38.83	28.18
C8-N7-C9-C10	138.16	153.38	138.81	142.49
C11-C12-C13-C14			141.96	148.95

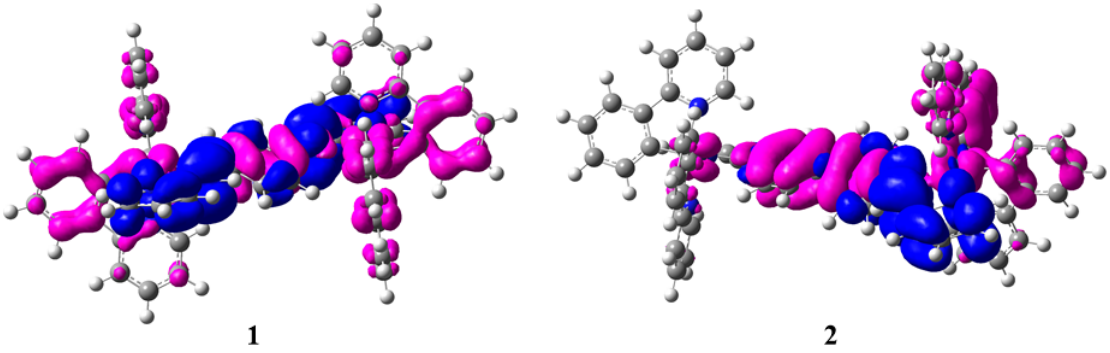

Fig. S15 Total electron density difference map for **1** and **2** in their T_1 geometries. Purple and blue colors show regions of decrease and increase in electron density, respectively.

8. References

1. N. M. Shavaleev, Z. R. Bell. G. Accorsi and M. D. Ward, *Inorg. Chim. Acta,* 2003, **351**, 159–166.

2. M. J. Frisch, G.W. Trucks, H. B. Schlegel, G. E. Scuseria, M. A. Robb, J. R. Cheeseman, G. Scalmani, V. Barone, B. Mennucci, G. A. Petersson, H. Nakatsuji, M. Caricato, X. Li, H. P. Hratchian, A. F. Izmaylov, J. Bloino, G. Zheng, J. L. Sonnenberg, M. Hada, M. Ehara, K. Toyota, R. Fukuda, J. Hasegawa, M. Ishida, T. Nakajima, Y. Honda, O. Kitao, H. Nakai, T. Vreven, J. A. Montgomery, Jr., J. E. Peralta, F. Ogliaro, M. Bearpark, J. J. Heyd, E. Brothers, K. N. Kudin, V. N. Staroverov, R. Kobayashi, J. Normand, K. Raghavachari, A. Rendell, J. C. Burant, S. S. Iyengar, J.

Tomasi, M. Cossi, N. Rega, J. M. M. Millam, M. Klene, J. E. K. Knox, J. B. C. Cross, V. Bakken, C. Adamo, J. Jaramillo, R. Gomperts, R. E. Stratmann, O. Yazyev, A. J. Austin, R. Cammi, C. Pomelli, J. W. Ochterski, R. L. Martin, K. Morokuma, V. G. Zakrzewski, G. A. Voth, P. Salvador, J. J. Dannenberg, S. Dapprich, A. D. Daniels, O. Farkas, J. B. Foresman, J. V. Ortiz, J. Cioslowski and D. J. Fox, Gaussian 09, Revision A.02, Gaussian, Inc, Wallingford CT, 2009.